Closed-loop deep borehole heat exchanger: Newcastle Science Central Deep Geothermal Borehole

Isa Kolo[1], Christopher S. Brown[1], Gioia Falcone[1], David Banks[1]

[1] James Watt School of Engineering, University of Glasgow, Glasgow, G12 8QQ

Isa.Kolo@glasgow.ac.uk

Keywords: Deep borehole heat exchanger, Closed-loop geothermal system, Single well, Repurposing, Finite element, Heterogeneous thermal conductivities, Newcastle Science Central Deep Geothermal Borehole, Newcastle Helix, OpenGeoSys.

ABSTRACT

In the effort to mitigate climate change, the UK is pursuing a low-carbon economy aimed at reducing greenhouse gas emissions to net zero by 2050. A key strategy in this drive is increasing the share of renewable energy sources. Deep (>500 m) geothermal energy has significant potential to decarbonise heat, but has been largely under-exploited in the country, partially due to perceived risk profile and high initial drilling cost. The latter might be offset by repurposing existing wells, including abandoned hydrocarbon wells (although these are associated with specific risks and challenges). The Newcastle Helix – a hybrid state-of-the-art city quarter at the heart of Newcastle – has an existing geothermal exploration borehole of 1.6 km depth, which could be repurposed as a single-well closed-circulation geothermal system. In this paper, numerical modelling of the Newcastle Science Central Deep Geothermal Borehole is presented, aiming to simulate its thermal response in the hypothetical case of its refurbishment as a closed-loop deep borehole heat exchanger. This study is part of the ongoing "NetZero GeoRDIE – Net Zero Geothermal Research for District Infrastructure Engineering" project.

1. INTRODUCTION

In 2019, in response to recommendations from the Committee on Climate Change, the UK became the first major economy to legislate for net zero greenhouse gas emissions by 2050 (Gov.uk, 2019). Heating the c.a. 30 million buildings in the UK contributes to 25% of all UK emissions, as fossil fuels are still being burned to generate the required energy (BEIS, 2021; Goodright, 2014). Hence, for the UK to meet its commitment to net-zero, decarbonisation of heating is essential. A key approach to achieve this is by using geothermal energy which is readily available all year round and is independent of weather conditions. Moreover, the UK has great geothermal energy potential from deep sedimentary basins, radiogenic granites, and shallower flooded mines (Gluyas *et al*., 2018). Geothermal energy can be harnessed for direct use and electricity generation; however, barriers to development remain, such as the high geological risk and initial drilling costs, which limit its adoption at scale (Soltani *et al.*, 2021).

In conventional geothermal exploitation, hot fluids are abstracted from production wells (e.g., Brown *et al*., 2022a), and the heat is transferred from the fluid to the user (e.g., Brown *et al*., 2022b). The thermally spent fluid may be disposed at surface but is often reinjected back into the subsurface via reinjection wells. Sometimes, hydraulic stimulation of the reservoir is needed to enhance well productivity or injectivity or to create subsurface flow pathways (e.g., enhanced geothermal system – EGS). These types of systems also present challenges, such as the risk of inducing seismic activity (Pasqualetti, 1980; Bayer *et al*., 2013). Some of these concerns are eliminated when a single-well closed-loop borehole heat exchanger is used, i.e., fluid is injected and extracted through a single, closed well-bore without direct interaction with the reservoir. Here, the fluid is predominantly heated by conduction through the borehole walls.

One such system which is increasingly gaining attention is the deep (coaxial) borehole heat exchanger (DBHE) system (e.g., Brown *et al*., 2021; Doran *et al.*, 2021; Renaud *et al.*, 2021). In this system, a concentric tube is inserted into the borehole; a circulating working fluid enters through the annulus and is heated via conduction by the surrounding rock before returning through a central "coaxial" extraction pipe (Fig. 1 – note that the opposite flow polarity may also be used). There is often a cementitious grout material between the various borehole casing strings and the formation to stabilise the borehole and prevent uncontrolled fluid ingress from the formation. Existing wells (such as hydrocarbon wells, dry exploration wells and unsuccessful conventional geothermal wells) lend themselves to being repurposed as DBHEs for geothermal energy extraction (Watson *et al*., 2020).

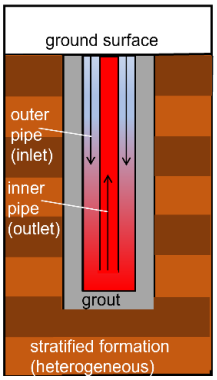

Figure 1: Sketch of a DBHE showing the borehole casing (outer pipe) and the central coaxial pipe (inner pipe)

In 2011, a geothermal exploration well was drilled in Newcastle targeting the underlying Fell Sandstone Formation (Fig. 2) (Younger *et al.*, 2016). The Newcastle Science Central Deep Geothermal Borehole (NSCDGB) revealed a high downhole temperature of up to 73°C, but the lower-than-expected hydraulic conductivity prevented the use of the borehole for conventional geothermal operation. The well is located within Newcastle Helix, which is a 24-acre hybrid city quarter in the centre of Newcastle (Newcastle Helix, 2022) and the EPSRC-funded project "NetZero GeoRDIE – Net Zero Geothermal Research for District Infrastructure Engineering" (Grant number EP/T022825/1) (GOW, 2020) set out to explore options for repurposing the well as a DBHE system.

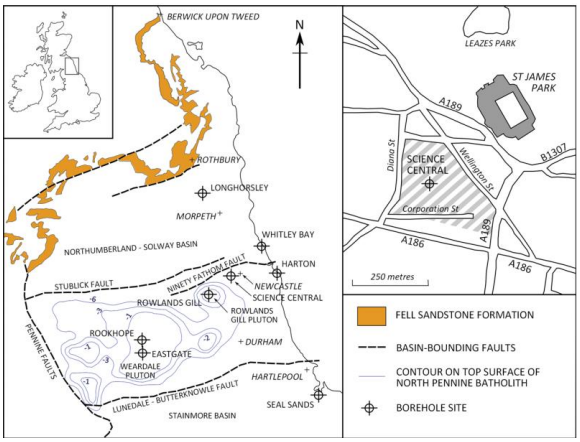

Figure 2: Map of Nort-East England showing the location of the NSCDGB and the principal geological features (Younger *et al.* (2016))

Although there is extensive literature on DBHEs, only few operational systems have been implemented (Sapinska-Sliwa *et al.*, 2016; Wang *et al.*, 2017; Falcone *et al.*, 2018). Numerical investigations can aid preliminary assessment of the potential of DBHEs and reduce the associated envelope of uncertainty. Different numerical modelling approaches have been developed using finite difference, finite volume and finite element methods.

In this study, we adopt the finite element method (FEM) to simulate the response of the NSCDGB in the hypothetical case of its refurbishment as a DBHE. We use a model developed with OpenGeoSys (OGS) (Chen *et al.*, 2019) - an open-source multi-physics simulation tool - to study heat extraction for one heating season (6 months). The influence of domain (rock) boundary conditions, diameter and material of the inner pipe, and different heat loads is investigated.

2. METHODS

For the FEM model of the DBHE, a 'dual-continuum' approach is adopted (Chen *et al.*, 2019) due to its computational efficiency. It considers the DBHE as a continuum using one-dimensional discretisation, while the surrounding rock is a second continuum, discretised using three-dimensional finite elements.

2.1 Governing Equations and Boundary Conditions

The DBHE has several casing and grout layers; however, we assume a simplified system with a single grout layer and a single casing (Fig. 1). As implemented in OGS, there are four heat transfer governing equations ([1], [4], [5] and [6]): for the rock formation, the grout, the borehole casing, and the central coaxial pipe. OGS considers both conduction and convection in the formation (Chen *et al.*, 2019):

$$\frac{\partial}{\partial t}\left[\phi\rho_f c_f + (1-\phi)\rho_r c_r\right]T_r + \nabla\cdot\left(\rho_f c_f \boldsymbol{q} T_r\right) - \nabla\cdot\left(\Lambda_r\cdot\nabla T_r\right) = H_r \quad [1]$$

where ϕ is the porosity of the rock, ρ is the density, T is the temperature and c is the specific heat capacity, with subscripts r and f representing the rock and circulating fluid respectively. All properties are assumed to be constant and independent of temperature and pressure. The Darcy fluid velocity is represented by $\boldsymbol{q}$. H_r is the source term and Λ_r is the thermal hydrodynamic dispersion tensor, which depends on the thermal conductivity of the rock λ_r :

$$\Lambda_r = \left[\phi\lambda_f + (1-\phi)\lambda_r\right]\boldsymbol{I} + \rho_f c_f\left[\alpha_T\|\boldsymbol{q}\|\boldsymbol{I} + (\alpha_L - \alpha_T)\frac{\boldsymbol{q}\otimes\boldsymbol{q}}{\|\boldsymbol{q}\|}\right] \quad [2]$$

with α_T and α_L representing the transverse and longitudinal thermo-dispersivity respectively, and $\boldsymbol{I}$, the unit identity matrix. A heat flux (q_n) boundary condition is adopted between the rock and the DBHE, given by:

$$q_{nT_r} = -(\Lambda_r\cdot\nabla T_r) \quad [3]$$

It is important to note that while OGS can consider both rock conduction and convection, only conduction is considered in this study, since we assumed that groundwater advection is negligible. Conduction dominates in the grout:

$$(1-\phi_g)\rho_g c_g \frac{\partial T_g}{\partial t} - \nabla \cdot \left[(1-\phi_g)\lambda_g \cdot \nabla T_g\right] = H_g \quad [4]$$

where the subscript g represents grout. In the borehole casing (i.e., inlet, subscript i) and central coaxial pipe (i.e., outlet, subscript o), heat transfer is governed by the following equations respectively:

$$\rho_f c_f \frac{\partial T_i}{\partial t} + \rho_f c_f \boldsymbol{v}_i \cdot \nabla T_i - \nabla \cdot (\Lambda_f \cdot T_i) = H_i \quad [5]$$

$$\rho_f c_f \frac{\partial T_o}{\partial t} + \rho_f c_f \boldsymbol{v}_o \cdot \nabla T_o - \nabla \cdot (\Lambda_f \cdot T_o) = H_o \quad [6]$$

in which $\boldsymbol{v}_i$ and $\boldsymbol{v}_o$ are the inlet and outlet fluid velocity vectors respectively; Λ_f is the hydrodynamic thermo-dispersion tensor expressed as:

$$\Lambda_f = \left(\lambda_f + \rho_f c_f \alpha_L \left\|v_f\right\|\right)\boldsymbol{I} \quad [7]$$

Horizontally, the thermal resistance to heat flow within the DBHE is analysed analogous to a resistor network, such that there is a thermal resistance to heat flow between: the rock and grout (R_{gr}), the grout and the borehole casing (R_{fig}) and the borehole casing and the central coaxial pipe (R_{ff}). These thermal resistances influence the boundary conditions at the interfaces where they exist. Based on their outer surface area of influence, they are expressed as heat transfer coefficients (Φ) which appear in the boundary conditions for the grout, borehole casing, and central coaxial pipe. The boundary condition for equation [4] is expressed as:

$$q_{nT_g} = -\Phi_{gr}(T_r - T_g) - \Phi_{fig}(T_i - T_g) \quad [8]$$

Similarly, the boundary conditions for equations [5] and [6] are respectively:

$$q_{nT_i} = -\Phi_{fig}(T_r - T_i) - \Phi_{ff}(T_o - T_i) \quad [9]$$

$$q_{nT_o} = -\Phi_{ff}(T_i - T_o) \quad [10]$$

In equations [8-10], the heat transfer coefficients are a function of the borehole casing diameter (d_{casing}), the central coaxial pipe diameter ($d_{central}$), and the borehole diameter (D_b) (including the grout), see Fig 1. The expressions for the heat transfer coefficients are: $\Phi_{gr} = 1/R_{gr}\pi D_b$, $\Phi_{fig} = 1/R_{fig}\pi d_{casing}$, and $\Phi_{ff} = 1/R_{ff}\pi d_{central}$. For how to compute the thermal resistances, see for example, Diersch *et al*. (2011).

Equations [1], [4], [5], and [6] are solved using the finite element method. After dividing the domain into finite elements, a test function is used to obtain a weak form of the equations which is integrated by parts. The primary variables are then discretised using shape functions to obtain the solution. For the time discretisation, Backward Euler finite difference discretisation is used (Diersch *et al*., 2011). This solution procedure has been implemented in OpenGeoSys Version 6 which is the software employed in this work. Mass balance has not been considered in this study and hence hydraulic considerations are not inherently incorporated.

2.2 Model Set-up and Pre-processing

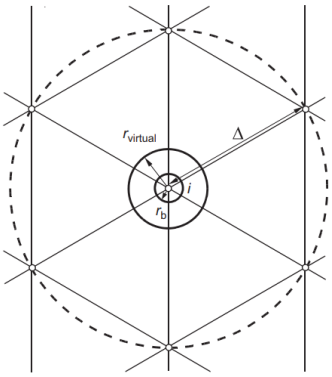

Figure 3: Spatial discretisation around DBHE node 'i' for n=6 (Diersch *et al*., 2011)

OGS can model a homogeneous formation as well as a heterogeneous stratified formation; the latter is adopted here. A suitable platform compatible with OGS Version 6 is needed to generate domain geometry and mesh before a finite element simulation. The free meshing tool Gmsh (Geuzaine and Remacle, 2009) can be used for this purpose. However, care must be taken when generating the mesh around the DBHE node (node *i* in Fig. 3). The DBHE has a one-dimensional representation, and the nodes (in the formation) next to the DBHE need to be at an optimum distance to ensure accuracy (Diersch *et al*., 2011). This is because, when the source term is applied to the DBHE node, it is not applied to the actual borehole radius (r_b). Rather, it is applied over a virtual radius ($r_{virtual}$) which is greater than r_b. The value of $r_{virtual}$ depends on the discretisation around the DBHE node represented by the nodal distance Δ, see Fig 3. Thus, Δ should be chosen so that, as close as possible, $r_{virtual} = r_b$. This can be achieved by adopting an optimal mesh distance given by Diersch *et al*. (2011):

$$\Delta = a r_b \quad [11]$$

where a depends on the number of nodes (n) surrounding the DBHE. For $n = 6$, $a = 6.13$.

A freely available pre-processing tool (bhe_setup_tool.exe) has been developed for OGS which uses Gmsh to automatically generate a multi-layered mesh while accounting for the optimal mesh distance from the DBHE node (Shao *et al*., 2016). It generates a geometry file (*.gli) and a mesh file (*.msh). This significantly simplifies pre-processing

since only input parameters are needed for mesh generation. The only obstacle is that the outputs are only compatible with OGS Version 5. To make them compatible with Version 6, the geometry file needs to be converted from a *.gli file to a *.gml file. This is best achieved using the application convertGEO.exe released with OGS version 6.0.8. The mesh file must also be converted from a *.msh file to a *.vtu file. This can be done by using the freely available interactive graphical user interface software GINA, see Jang *et al.* (2017).

3. APPLICATION TO THE NSCDGB

The geological and thermal properties of the various strata have been extracted from Younger *et al.* (2016) (Fig. 4, Table A). For properties that were not reported, other sources have been sought, as summarised below.

3.1 Stratigraphy and Parametrisation

The total depth of the NSCDGB is 1820m, with a 7-inch casing stopping at 941m and a 6-inch (nominal) diameter hole extending to the total depth. A 4.½-inch Techniseal liner was inserted from 922 to 1651 m. A schematic of the successive formations of Carboniferous age from ground level down to 1651m is shown in Fig. 4 (Younger *et al.*, 2016). Estimates of the geothermal gradient and thermal conductivities of the geological layers intersected by the borehole were also presented by Younger *et al.* (2016) from the Stainmore Formation (500m) to the bottom of the borehole. Above the Stainmore Formation, and for other parameters such as specific heat capacity, density, and porosity, it became necessary to turn to other sources, such as Westaway (2020) and Banks (2021).

The Coal Measures have been assumed to consist of 34% sandstone, 33% siltstone and 33% mudstone. Thus, their densities, specific heats and porosity have been estimated based on weighted averages from values by Rollin (1987), Armitage *et al.* (2016) and Jones *et al.* (2000). Representative values for properties of siltstone have been obtained from Eppelbaum *et al.* (2014), Kang *et al.* (2011) and Morris and Johnson (1967). For sandstone, density, porosity and specific heat values have been assumed for the Millstone Grit Group, Tyne Limestone and Fell Sandstone formations; for Stainmore Formation, Alston Formation and the Fault Zone, properties of limestone have been assumed although successions of mudstone, siltstone and mudstone are present. Values of density have been obtained from Kimbell *et al.* (2006) and the geothermal gradient was taken from Gebski *et al.* (1987). A surface temperature of 9°C is assumed with a geothermal gradient of 33.4°C/km (Gebski *et al.*, 1987).

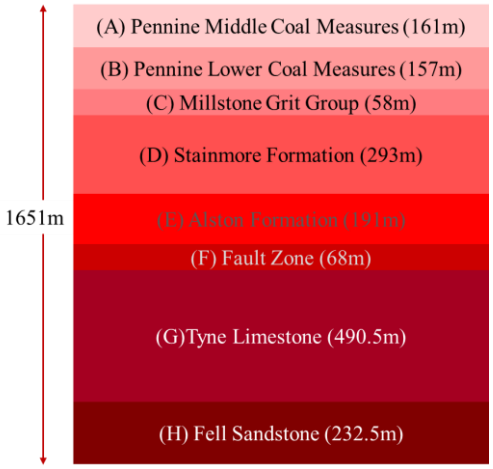

Figure 4: The stratigraphy of NSCDGB showing different formations and their thicknesses up to 1651m depth (after Younger *et al.* (2016))

Table A: Parameters of different formations (layers) for the NSCDGB.

Layer	Thermal Conductivity [W/m/°C]	Density [kg/m^3]	Porosity	Specific Heat [J/kg/° C]
A	2.35	2451	0.11	857.4
B	2.35	2451	0.11	857.4
C	2.9	2460	0.156	930
D	2.613	2500	0.018	1000
E	2.627	2500	0.018	1000
F	2.75	2500	0.018	1000
G	2.857	2460	0.156	930
H	2.913	2460	0.156	930

For the operation of the DBHE, fresh water is assumed as the circulating fluid. The grout is assumed to be an API Grade G water-saturated cement grout. The annular casing (outer pipe) is assumed to be made of steel, while the central coaxial pipe is assumed to be made of high-density polyethylene (HDPE). A borehole depth of 1651m and borehole diameter of 0.216m have been adopted, with a casing outer diameter of 161.7mm and central coaxial pipe outer diameter of 100.5mm for the DBHE (Banks, 2021). Table B shows other parameters adopted for the DBHE system. The reference temperature is the initial central coaxial pipe fluid inlet temperature (t=0) when adopting a power-controlled solution. We note that, to achieve this configuration down to 1651 m, the installed 4½-inch Techniseal liner would need to be removed. A circulation rate of 8.33 kg/s was assumed, which is high enough to ensure optimum and sustained extraction, although it could result in high pressure losses during circulation, which is not modelled in this study.

Table B: Modelled parameters for the NSCDGB DBHE System

Parameter	Value	Unit
Outer diameter of outer pipe	177.9	mm
Outer diameter of inner pipe	100.5	mm
Outer pipe wall thickness	8.1	mm
Inner pipe wall thickness	6.88	mm
Initial surface temperature	9	°C
Reference temperature	9	°C
Geothermal gradient	33.4	K/km
Fluid flow rate	8.33	kg/s
Dynamic viscosity of fluid	0.0008	Pa·s
Fluid volumetric heat capacity	4.158	MJ/m^3/K
Grout volumetric heat capacity	1.824	MJ/m^3/K
Fluid thermal conductivity	0.59	W/(m·K)
Grout thermal conductivity	1.05	W/(m·K)
Inner piper (HDPE) thermal conductivity	0.45	W/(m·K)
Outer pipe thermal conductivity (Steel)	52.7	W/(m·K)

3.2 Geometry, Initial and Boundary Conditions

After identifying parameters to work with for the formation and the DBHE system, bhe_setup_tool.exe was used to generate the geometry and convert the files to make them compatible with OpenGeoSys Version 6. A domain of size 100m × 100m × 1807m (x, y, z) is adopted. Based on the surface temperature and geothermal gradient, the initial temperature for the formation is given by

$$T = 9 + 0.0334z \qquad [12]$$

in °C where z (positive) represents depth. A linear geothermal gradient has been assumed for simplicity, although Younger *et al*. (2016) show a near-linear geothermal gradient to depths of ~1800 m. The meshed geometry is shown in Fig 5. The DBHE is centralised within the formation.

The constant temperature (Dirichlet) boundary conditions for the 6 faces of the rock (formation) also follow equation [12]. To implement the initial temperature of the formation (with geothermal gradient) in OGS, the *.vtu mesh file is imported into ParaView, and the calculator function is used with the scalar array values 'CoordsZ'. To implement the boundary conditions, one approach is to use the OpenGeoSys application ExtractSurface.exe. This extracts each of the 6 faces (top, bottom and 4 lateral) on the boundaries into a separate *.vtu file. Each file is then imported into ParaView to apply the Dirichlet temperature boundary condition using the calculator function.

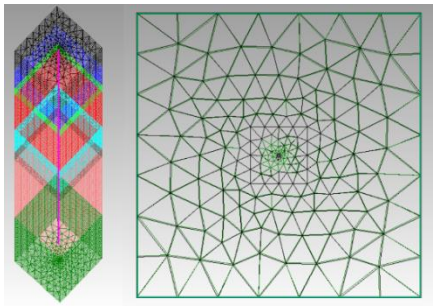

Figure 5: Meshed domain showing different layers: side view (left); top view (right). The DBHE is the pink line (one-dimensional discretisation).

3.3 Model Verification

The model is compared against a finite difference implementation of the dual-continuum approach presented by Brown *et al*. (2021). This is a MATLAB implementation that was originally developed to investigate deep borehole heat exchangers in the Cheshire Basin. This MATLAB model has been developed further to incorporate heterogeneities, such that an identical model was set-up to OGS. To compare the current OGS model and the MATLAB model, only a depth of 922m is considered for the DBHE, considering that the 4½ Techniseal tubing after 922m makes it practically difficult to reach higher depths. The OGS domain size is 100m ×100m and 1418.5 m deep. A one-year period is considered with 6-month injection of hot water for storage at 95°C followed by another 6-month injection of cold water at 10°C to extract heat. A mass flow rate of 8.33 kg/s is maintained. Due to stability limitations of the finite difference method, a constant timestep of 15s is used. The finite element discretisation in OGS allows large time steps to be used; variable timesteps with a maximum timestep of 50,000s were used.

The outlet temperature result is plotted in Fig 6 for both MATLAB and OGS. The results show good agreement with less than 0.1°C difference between the two models. At the end of the 6-month injection period, some heat has been stored in the formation since the temperature (88.48°C) is well below the injection temperature of 95°C. Again, at the end of the extraction period, the injected water flows out at 11.82 °C, indicating some heat gain. Heat injected during charging is 991.4 MWh, representing an average rate of -226.97 kW. Heat gained during extraction is 276.7 MWh, representing an average rate of 63.36 kW.

A more practical operation scenario is when the extracted heat load is kept constant so that the inlet and outlet temperatures fluctuate to maintain the heat load. To simulate this scenario, a 50kW load is applied. The two models are again compared, as shown in Fig. 7. Both inlet and outlet temperatures show good

agreement with little difference (typically, within 0.25°C) between the two models. The OGS model performs well and can thus be employed for further study of a DBHE system for the Newcastle Helix.

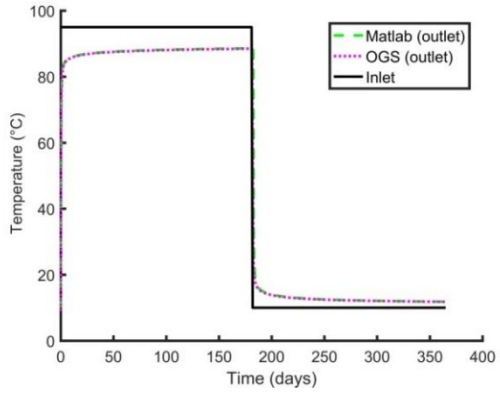

Figure 6: Comparison of outlet temperature between MATLAB and OGS.

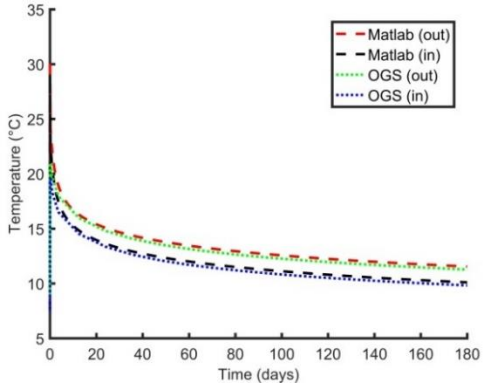

Figure 7: Comparison between MATLAB and OGS for 50kW heat load. The average formation temperature is 24.36°C.

4. RESULTS AND DISCUSSION

Only a period of one heating season (~ 6 months) is considered in the simulations for the Newcastle Science Central Deep Geothermal Borehole. The domain and other computational parameters are as used in the verification (section 3.3). For a 50kW load, the effects of the rock boundary condition, and different proposed central pipe diameters is probed. Then, varying heat loads are considered.

4.1 Formation (Rock) Boundary Conditions

One applicable procedure for implementing boundary conditions for the rock in OGS has been discussed (section 3.2). In this section, we look at how important this is for the simulations. Although largely dependent on the aims of the analysis or research, the primary outputs from the simulations of a DBHE tend to be the fluid inlet and outlet temperatures. With a 50kW heat load applied, a scenario with homogeneous Neumann boundary condition at the rock boundaries is tested: $\nabla T = 0$. This implies that for the top, bottom and lateral boundaries, there is no heat flux (NHF Boundary Condition). This is compared with the case of Dirichlet-type constant temperature (CT) boundary conditions on all boundaries.

Results are shown in Fig. 8 for inlet and outlet fluid temperatures at the well head (borehole top). There is no noticeable difference between the results for NHF and CT boundary conditions. The boundary conditions do not affect the circulation fluid temperatures. Fig. 9 shows the grout and rock temperatures for the different boundary conditions considered. With a constant temperature (CT) boundary condition, the surface temperature remains constant while the surface temperature varies significantly when zero heat flux (NHF) is imposed on the top boundary.

The results in Fig 8. show a sharp decrease in temperature within the first 60 days ($\Delta T \approx 8$°C) and then a small decrease $\Delta T \approx 2$°C from 60 – 174 days. With time, temperature drop reduces such that continuous extraction only has a minor impact on the inlet and outlet temperatures. Between the inlet and outlet fluid, a constant ΔT of 1.44°C has been imposed. This is imposed to account for a constant heat flux of 50 kW as the mass flow rate and the thermal capacity are fixed.

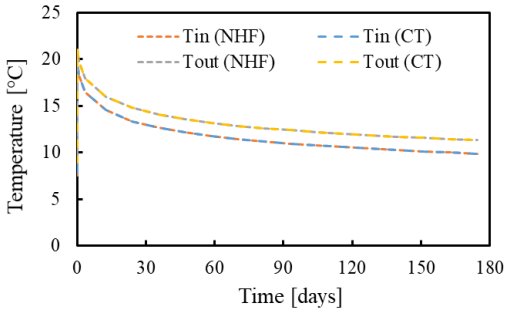

Figure 8: Comparison of inlet and outlet fluid temperatures for 50kW heat load simulations while imposing no heat flux boundary condition (NHF) and constant temperature boundary condition (CT). Results are presented at the borehole head (z=0).

Fig. 10 presents the rock formation from a section through plane y = 0 showing the centralised DBHE. To look at the rock temperature more closely, it is plotted across the width along the line z = −463.9m on the plane y=0. Results are shown in Fig. 11 for time t =174 days. The initial rock temperature (24.5°C) is also plotted for reference. The temperature effect is felt up to a radial distance of ~13m. However, beyond this point, the formation temperature remains undisturbed. This explains why the rock boundary conditions have no effect on the fluid inlet and outlet temperatures. Provided the domain boundary is beyond this area of influence (13m), the temperatures within the DBHE will not be significantly affected. Hence, the rock temperature with no heat flux and constant temperature boundary conditions remains the same.

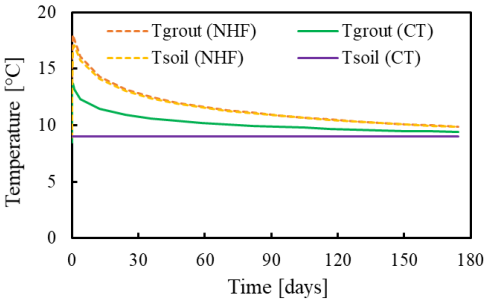

Figure 9: Comparison of grout and rock temperatures for 50kW heat load simulations while imposing no heat flux boundary condition (NHF) and constant temperature boundary condition (CT). Results are presented at the borehole head (z=0).

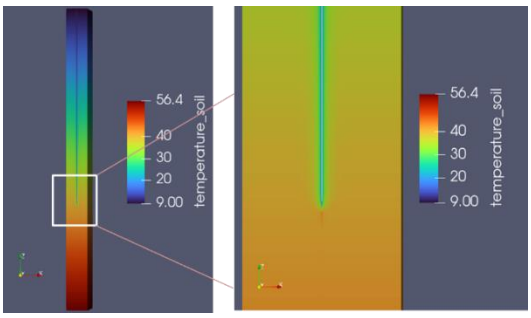

Figure 10: Computational domain showing rock temperature at time, t=174 days: A cross-section through the x-z plane at y=0. Results for time t = 174 days.

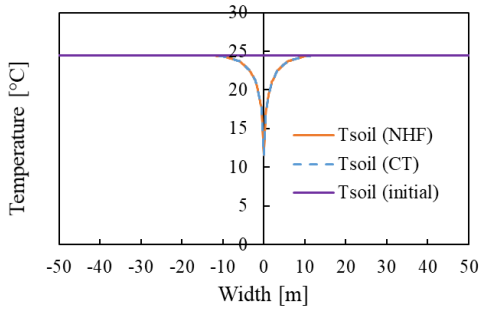

Figure 11: Rock temperature for simulation with no heat flux (NHF) and constant temperature (CT) boundary conditions at z = −463.9m along the mid x-z plane. Results at time t = 174 days.

The fluid inlet and outlet temperatures are plotted along the DBHE depth at time t = 174 days on Fig. 12. Again, the same fluid temperatures are observed for both boundary conditions considered. As seen on Fig. 12, after 174 days, the fluid injected at 9°C reaches 11.86°C at the bottom of the DBHE due to conduction from surrounding formation, a gain of 2.86°C. The fluid exits at 11.3°C, so about 0.56°C is lost on the fluid return from the bottom to the top of the DBHE.

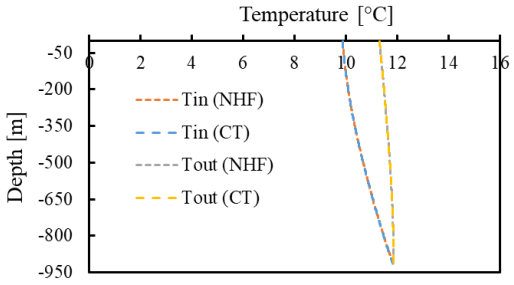

Figure 12: Inlet and outlet temperatures along BHE depth for simulations with no heat flux (NHF) and constant temperature (CT) boundary conditions. Results at time t = 174 days.

To analyse the heat transfer across rock layers, we use the negative change in temperature between grout and rock $(T_g - T_r)$ since it is proportional to the heat transfer (conduction heat transfer). Fig. 13 shows the thermal conductivities of rock layers and the corresponding change in temperature. With an increase in thermal conductivity, heat transfer increases and so does the change in temperature (in the negative direction).

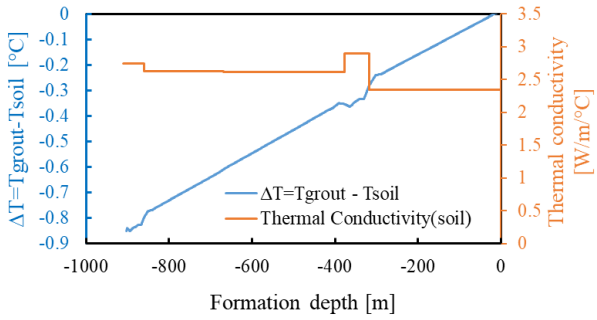

Figure 13: Change in temperature between rock and grout and thermal conductivity along BHE depth at time t = 174 days.

4.2 Central Coaxial Pipe Material and Diameter

Hydraulic design considerations have shown that the central pipe should have an outer diameter of 75mm or more (Banks, 2021). So far, the central pipe has been assumed to be made of HDPE with an outer diameter of 100.5mm. The effect of changing the central coaxial (outlet) pipe diameter is now investigated. Three values have been considered – a diameter (D) of 61.4mm (6.8mm thickness), 73.6mm (9=8.2mm wall thickness) and 90 mm (10mm wall thickness).

Results are shown in Fig. 14 at the top of the borehole. No significant difference is seen for the different pipe diameters. At 174 days, the outlet temperature is 11.31°C for the reference value of D = 100.5 mm. For D = 90mm, the outlet temperature is 11.43°C which represents a very marginal increase. For D = 61.4 mm and D= 73.6mm, the outlet temperature is 11.42°C, all at time t = 174 days. While the effects on temperature

appear low, the influence of different diameters is likely to impact the hydraulic operation of the deep BHE.

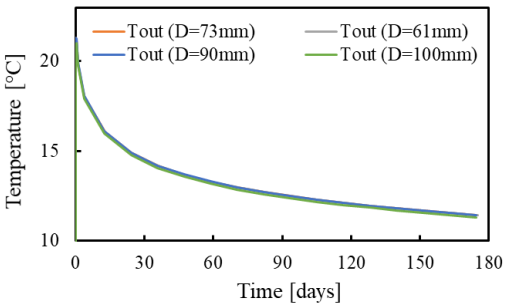

Figure 14: Outlet fluid temperatures considering different values of the inner diameter of the inner pipe. Results at z = 0m.

Li *et al.* (2021) tried different materials for the central pipe of a DBHE and while a polyvinylchloride (PVC) pipe gave the best performance, it was not recommended because it cannot withstand high temperatures and is susceptible to leak and wear. Instead, they recommended a polypropylene (PP-R) pipe which has a thermal conductivity of 0.24 W/(m·°C). We investigate the effect of using PP-R instead of HDPE which has a thermal conductivity of ~0.45 W/(m·°C). Outlet fluid temperatures are shown in Fig. 15 for a 174-day period (D=100.5mm). It is seen that PP-R does give higher output temperatures due to its slightly lower thermal conductivity. However, the increase is marginal. At 174 days, the outlet temperature is 11.47°C compared to 11.31°C for HDPE – a 0.16°C increase.

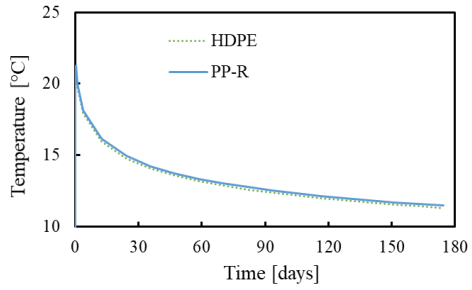

Figure 15: Comparison of outlet fluid temperatures for a central pipe made of PP-R vs a HDPE central pipe.

A little after two months, the inlet and outlet fluid temperatures are plotted in Fig. 16 at 70 days. This is at a time when temperatures are relatively higher compared to Fig. 12. It is seen that for both the HDPE and the PP-R pipe, the temperature change (ΔT) at the top remains the imposed 1.44°C. However, even though the HDPE pipe reaches a slightly higher temperature at depth, it loses more heat before reaching the surface. The PP-R pipe has an outlet fluid temperature of 13°C compared to 12.86°C for the HDPE pipe. This corroborates findings from Dijkshoorn *et al.* (2014) who show that with increasing flow rate, the importance of inner pipe insulation decreases. Considering the marginal difference in performance, factors like economics of using both pipes might be more important to guide the design process.

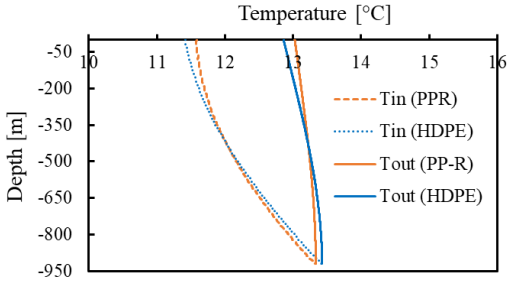

Figure 16: Inlet and outlet temperatures along BHE depth for a central pipe made of HDPE vs central pipe made of PP-R. Results are shown at time t = 70 days.

4.3 Varying Heat Load

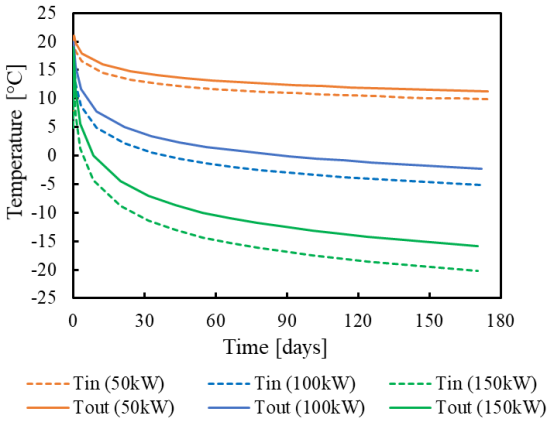

Figure 17: Inlet and outlet fluid temperatures for different heat loads.

A heat load increase is considered to check the performance of the DBHE. Two notional cases of 100kW and 150kW heat load have been simulated. Results showing the inlet and outlet fluid temperatures are shown in Fig. 17. While the temperature change for the 50kW load is ΔT = 1.44°C, the 100kW load requires ΔT = 2.89°C and the 150kW load requires ΔT = 4.33°C. The DBHE can supply a 50kW load with the flow temperature not going below 9.8°C after 174 days. For a 100kW load, the flow temperature goes below 0°C after ~44 days. The freezing point of water is 0°C and reaching this temperature will cause a lot of challenges for the DBHE operation. Hence, it is reasonable to design a DBHE operation following this criterion. Based on this, the DBHE cannot supply a 100kW load. For the 150kW load, the flow temperature goes below

0°C after just 8 days. The DBHE appears to be able to support a 50kW heat load.

5. CONCLUSIONS AND OUTLOOK

In this study, the response of the NSCDGB in the hypothetical case of its refurbishment as a DBHE has been investigated. A model based on the multi-physics finite element software OGS (Version 6) has been developed taking the stratigraphy of the Newcastle area into account. The dual-continuum approach with one-dimensional discretisation for the BHE and three-dimensional discretisation for the surrounding formation (rock) has been adopted. Simulations have been performed for a 174-day period to give insights into the operation of the BHE as a deep coaxial borehole heat exchanger.

Results show that the DBHE can provide around 50kW heat load for 174 days without going below 9°C. The effect of imposing Dirichlet boundary conditions on the boundaries of the rock domain has been analysed. While the temperature of the rock and grout might differ based on the imposed boundary conditions, the inlet and outlet flow temperatures tend to be unaffected by the rock boundary conditions provided the surrounding rock domain boundary is outside the region of influence of the DBHE temperature diffusion (~13m for the considered simulations). The outer diameter of the central BHE pipe has no significant thermal effect for the practical values considered in this study, but hydraulic effects could be significant. Plastic is preferred on thermal grounds to steel for the central (coaxial) pipe, due to its lower thermal conductivity and lower thermal short-circuiting. Of the plastics, PP-R performs slightly better than HDPE, but with only a modest overall temperature gain (c. 0.16°C) in the fluid temperature.

While the preliminary simulations suggest that a heat load of 100kW could not be supplied by the DBHE for an entire heating season, further simulations will be required to ascertain the maximum short term peak load, and for how long a 50kW heat load could be sustained. Effect of flow rate and accessible borehole depth must also be assessed. Lastly, this study has only considered the subsurface potential, but coupling with a surface demand model (e.g., using TESPy, see Cai *et al*., 2022) is needed for a whole-system approach.

Acknowledgements

This work was supported by the UK Engineering and Physical Sciences Research Council (EPSRC) grant EP/T022825/1. The first author wishes to thank Dr. Chaofan Chen of the Helmholtz Centre for Environmental Research for the valuable discussions on relevant OpenGeoSys 6 features.

REFERENCES

Armitage, P. J., Worden, R. H., Faulkner, D. R., Butcher, A. R., & Espie, A. A. (2016). Permeability of the Mercia Mudstone: suitability as caprock to carbon capture and storage sites. *Geofluids*, *16*(1), 26-42.

Banks, D., 2021. Thermal properties of well construction materials - Newcastle Science Central borehole. Internal University of Glasgow report for GOW (2020).

Bayer, P., Rybach, L., Blum, P., & Brauchler, R. (2013). Review on life cycle environmental effects of geothermal power generation. *Renewable and Sustainable Energy Reviews*, *26*, 446-463.

BEIS (2021). Heat and buildings strategy. Presented to Parliament by the Secretary of State for Business, Energy and Industrial Strategy by Command of Her Majesty. October 2021

Brown, C.S., Cassidy, N.J., Egan, S.S. and Griffiths, D., 2022a. A sensitivity analysis of a single extraction well from deep geothermal aquifers in the Cheshire Basin, UK. *Quarterly Journal of Engineering Geology and Hydrogeology*.

Brown, C.S., Cassidy, N.J., Egan, S.S. and Griffiths, D., 2022b. Thermal and Economic Analysis of Heat Exchangers as Part of a Geothermal District Heating Scheme in the Cheshire Basin, UK. *Energies*, *15*(6), p.1983.

Brown, C. S., Cassidy, N. J., Egan, S. S., & Griffiths, D. (2021). Numerical modelling of deep coaxial borehole heat exchangers in the Cheshire Basin, UK. *Computers & Geosciences*, *152*, 104752.

Cai, W., Wang, F., Chen, S., Chen, C., Zhang, Y., Kolditz, O., & Shao, H. (2022). Importance of long-term ground-loop temperature variation in performance optimization of Ground Source Heat Pump system. *Applied Thermal Engineering*, 117945.

Chen, C., Shao, H., Naumov, D., Kong, Y., Tu, K., & Kolditz, O. (2019). Numerical investigation on the performance, sustainability, and efficiency of the deep borehole heat exchanger system for building heating. *Geothermal Energy*, *7*(1), 1-26.

Doran, H. R., Renaud, T., Falcone, G., Pan, L., & Verdin, P. G. (2021). Modelling an unconventional closed-loop deep borehole heat exchanger (DBHE): sensitivity analysis on the Newberry volcanic setting. *Geothermal Energy*, *9*(1), 1-24.

Diersch, H. J., Bauer, D., Heidemann, W., Rühaak, W., & Schätzl, P. (2011). Finite element modeling of borehole heat exchanger systems: Part 1. Fundamentals. *Computers & Geosciences*, *37*(8), 1122-1135.

Dijkshoorn, L., Speer, S., & Pechnig, R. (2013). Measurements and design calculations for a deep coaxial borehole heat exchanger in Aachen, Germany. *International Journal of Geophysics*, *2013*.

Eppelbaum, L., Kutasov, I., & Pilchin, A. (2014). *Applied geothermics* (p. 267). Springer Berlin Heidelberg.

Falcone, G., Liu, X., Okech, R.R., Seyidov, F. & Teodoriu, C. (2018) Assessment of deep geothermal energy exploitation methods: The need for novel single-well solutions. *Energy*, 160, 54-63.

Gebski, J.S., Wheildon, J., Thomas-Betts, A., (1987). Investigations of the UK heat flow field (1984-1987). Report WJ/GE/87/6, British Geological Survey, Nottingham, 60 pp

Geuzaine, C., & Remacle, J. F. (2009). Gmsh: A 3-D finite element mesh generator with built-in pre-and post-processing facilities. *International journal for numerical methods in engineering*, *79*(11), 1309-1331.

Gluyas, J. G., Adams, C. A., Busby, J. P., Craig, J., Hirst, C., Manning, D. A. C., ... & Younger, P. L. (2018). Keeping warm: a review of deep geothermal potential of the UK. *Proceedings of the Institution of Mechanical Engineers, Part A: Journal of Power and Energy*, *232*(1), 115-126.

Goodright, V. (2014). Estimates of heat use in the United Kingdom in 2013. *Department of Energy and Climate Change Statistics*.

GOW (2020). Grants on the web. EPSRC EP/T022825/1. Accessed April 1, 2022. https://gow.epsrc.ukri.org/NGBOViewGrant.aspx?GrantRef=EP/T022825/1

Gov.uk, (2019). UK becomes first major economy to pass net zero emissions law. Accessed April 1, 2022. https://www.gov.uk/government/news/uk-becomes-first-major-economy-to-pass-net-zero-emissions-law.

Jang, E., Boog, J., He, W., & Kalbacher, T. (2017). *OpenGeoSys Tutorial: Computational Hydrology III: OGS# IPhreeqc Coupled Reactive Transport Modeling*. Springer.

Jones, H. K., Morris, B. L., Cheney, C. S., Brewerton, L. J., Merrin, P. D., Lewis, M. A., ... & Robinson, V. (2000). The physical properties of minor aquifers in England and Wales.

Kang, H., Wu, Y., & Gao, F. (2011). Deformation characteristics and reinforcement technology for entry subjected to mining-induced stresses. *Journal of Rock Mechanics and Geotechnical Engineering*, *3*(3), 207-219.

Kimbell, G.S., Carruthers, R.M., Walker, A.S.D., Williamson, J.P., (2006). Regional geophysics of southern Scotland and northern England. Version 1.0 on CD-ROM. British Geological Survey, Keyworth. Available from: https://shop.bgs.ac.uk/Bookshop/product.cfm?p_id=KRGSCD

Li, G., Yang, J., Zhu, X., & Shen, Z. (2021). Numerical study on the heat transfer performance of coaxial shallow borehole heat exchanger. *Energy and Built Environment*, *2*(4), 445-455.

Newcastle Helix (2022). https://newcastlehelix.com/. Downloaded in April 2022.

Pasqualetti, M. J. (1980). Geothermal energy and the environment: The global experience. *Energy*, *5*(2), 111-165.

Renaud, T., Pan, L., Doran, H., Falcone, G., & Verdin, P. G. (2021). Numerical analysis of enhanced conductive deep borehole heat exchangers. *Sustainability*, *13*(12), 6918.

Rollin, K. E. (1987). Catalogue of geothermal dat for the land area of the United Kingdom. Third revision: April 1987. Investigation of the Geothermal Potential of the UK, British Geological Survey, Keyworth.

Sapinska-Sliwa, A., Rosen, M. A., Gonet, A., & Sliwa, T. (2016). Deep borehole heat exchangers—a conceptual and comparative review. *International Journal of Air-Conditioning and Refrigeration*, *24*(01), 1630001.

Shao, H., Hein, P., Sachse, A., & Kolditz, O. (2016). *Geoenergy modeling II: shallow geothermal systems*. Springer International Publishing.

Soltani, M., Kashkooli, F. M., Souri, M., Rafiei, B., Jabarifar, M., Gharali, K., & Nathwani, J. S. (2021). Environmental, economic, and social impacts of geothermal energy systems. *Renewable and Sustainable Energy Reviews*, *140*, 110750.

Wang, Z., Wang, F., Liu, J., Ma, Z., Han, E., & Song, M. (2017). Field test and numerical investigation on the heat transfer characteristics and optimal design of the heat exchangers of a deep borehole ground source heat pump system. *Energy conversion and management*, *153*, 603-615.

Watson, S. M., Falcone, G., & Westaway, R. (2020). Repurposing hydrocarbon wells for geothermal use in the UK: The onshore fields with the greatest potential. *Energies*, *13*(14), 3541.

Westaway, R. (2020). *Rock thermal properties for Newcastle Helix site*. Internal University of Glasgow report for GOW (2020).

Younger, P. L., Manning, D. A., Millward, D., Busby, J. P., Jones, C. R., & Gluyas, J. G. (2016). Geothermal exploration in the Fell Sandstone Formation (Mississippian) beneath the city centre of Newcastle upon Tyne, UK: the Newcastle Science Central deep geothermal borehole. *Quarterly Journal of Engineering Geology and Hydrogeology*, *49*(4), 350-363.